Acta Biomaterialia xxx (2012) xxx–xxx

Contents lists available at SciVerse ScienceDirect

Acta Biomaterialia

journal homepage: www.elsevier.com/locate/actabiomat

The effects of interactive mechanical and biochemical niche signaling on osteogenic differentiation of adipose-derived stem cells using combinatorial hydrogels

Michelle Nii [a,1], Janice H. Lai [b,1], Michael Keeney [c], Li-Hsin Han [c], Anthony Behn [c], Galym Imanbayev [e], Fan Yang [c,d,*]

[a] Program of Material Science and Engineering, Stanford University, Stanford, CA 94305, USA
[b] Department of Mechanical Engineering, Stanford University, Stanford, CA 94305, USA
[c] Department of Orthopaedic Surgery, Stanford University, Stanford, CA 94305, USA
[d] Department of Bioengineering, Stanford University, Stanford, CA 94305, USA
[e] Program of Human Biology, Stanford University, Stanford, CA 94305, USA

ARTICLE INFO

Article history:
Received 18 May 2012
Received in revised form 11 October 2012
Accepted 2 November 2012
Available online xxxx

Keywords:
Stem cells
Osteogenesis
Hydrogel
Combinatorial
Mechanical properties

ABSTRACT

Stem cells reside in a multi-factorial environment containing biochemical and mechanical signals. Changing biochemical signals in most scaffolds often leads to simultaneous changes in mechanical properties, which makes it difficult to elucidate the complex interplay between niche cues. Combinatorial studies on cell–material interactions have emerged as a tool to facilitate analyses of stem cell responses to various niche cues, but most studies to date have been performed on two-dimensional environments. Here we developed three-dimensional combinatorial hydrogels with independent control of biochemical and mechanical properties to facilitate analysis of interactive biochemical and mechanical signaling on adipose-derived stem cell osteogenesis in three dimensions. Our results suggest that scaffold biochemical and mechanical signals synergize only at specific combinations to promote bone differentiation. Leading compositions were identified to have intermediate stiffness (~55 kPa) and low concentration of fibronectin (10 μg ml^{-1}), which led to an increase in osteocalcin gene expression of over 130-fold. Our results suggest that scaffolds with independently tunable niche cues could provide a powerful tool for conducting mechanistic studies to decipher how complex niche cues regulate stem cell fate in three dimensions, and facilitate rapid identification of optimal niche cues that promote desirable cellular processes or tissue regeneration.

1. Introduction

Stem cells hold great promise for tissue regeneration due to their ability to self-renew and differentiate into specific tissue types. However, a long-standing bottleneck in the stem-cell-based approach to tissue regeneration is the lack of understanding of how stem cell fate is regulated in three dimensions. Stem cells reside in a highly complex niche in vivo where a variety of microenvironmental cues form an intertwined signaling regulatory network that maintains stem cell fate and function [1,2]. Both biochemical cues such as soluble growth factors and cytokines, extracellular matrix (ECM) molecules, as well as mechanical cues such as intrinsic matrix stiffness and extrinsic forces, are crucial regulators of stem cell fate [3]. Extensive studies have been performed to investigate how stem cells respond to individual types of microenvironmental cues. However, how the complex interplay among niche cues collectively influence stem cell fate and function remains largely unknown. Recently, combinatorial screening of stem cell interactions with material libraries has emerged as a novel approach to achieve rapid identification of optimal niche signals with reduced materials and costs [4–8]. These combinatorial screening studies showed that stem cells respond to interactive niche signals in a non-linear manner, highlighting the importance of examining the response of stem cells to interactive niche signals in a systematic manner to elucidate how they collectively regulate stem cell fate in vivo [4,5].

In conventional three-dimensional (3-D) culture systems, various microenvironmental cues are often intertwined and cannot be individually controlled. For instance, type I collagen is widely used for tissue engineering applications, but increasing its concentration to increase biochemical ligand density will also lead to simultaneous change in the mechanical stiffness of the matrix

* Corresponding author at: Department of Orthopaedic Surgery, Stanford University, Stanford, CA 94305, USA. Tel.: +1 650 725 7128; fax: +1 650 723 9370.
E-mail address: fanyang@stanford.edu (F. Yang).
[1] These authors contributed equally to this work.

1742-7061/$ - see front matter © 2012 Acta Materialia Inc. Published by Elsevier Ltd. All rights reserved.
http://dx.doi.org/10.1016/j.actbio.2012.11.002

[9,10]. Given the complex interplay among different microenvironmental cues, a 3-D culture system that allows for the independent control of individual microenvironmental cues would help elucidate how stem cells respond to interactive niche signals in three dimensions. Recent combinatorial screening studies on stem cell–niche interactions have shed light on stem cell–microenvironmental cue interactions. However, most work to date were conducted on two-dimensional (2-D) surfaces [4,6,7], while the architecture of the stem cell niche in vivo is three dimensional. Cells in the body reside in a 3-D environment and previous work has highlighted that cell behavior in three dimensions may vary significantly from cell behavior in two dimensions [11–13]. While 3-D combinatorial platforms have been developed to examine the effects of interactive biochemical cues on stem cell adhesion and differentiation [5,8], how biochemical cues interact with mechanical cues to regulate stem cell fate remains largely unknown. Recent studies have revealed the critical role of mechanical cues in directing stem cell differentiation [14]. In particular, matrix stiffness together with adhesion-ligand presentations has been shown to regulate stem cell fate in three dimensions [15,16]. However, platforms that allow the examination of stem cell responses to interactive biochemical and mechanical cues remain lacking.

The goal of this study is to develop novel 3-D combinatorial hydrogels with independent control of biochemical and mechanical properties to facilitate the analysis of interactive niche signaling on stem cell osteogenesis in three dimensions. We hypothesized that biochemical and mechanical cues of the microenvironment interact in a non-linear manner in regulating stem cell osteogenesis in three dimensions. To vary the mechanical properties of the hydrogels, poly(ethylene glycol) diacrylate (PEGDA) with varying molecular weight or concentration was used [17–19]. To vary the biochemical cues within the combinatorial hydrogels, different amounts of fibronectin (FN) and laminin (LN) were incorporated into the hydrogel network due to their importance in cell signaling and cell adhesion [5,20–25]. Type I collagen, the most abundant protein found in bone extracellular matrix, was included at a constant concentration to facilitate cell adhesion. We chose to examine the osteogenesis of adipose-derived stem cells (ADSCs) due to their relative abundance, ease of isolation and potential to differentiate into bone lineage [26,27]. ADSCs were encapsulated in combinatorial hydrogels for 21 days and outcomes were examined using gene expression, biochemical assays and immuonfluorescence staining. In addition, to examine the role of matrix stiffness on ADSC osteogenesis, blebbistatin, a small molecule inhibitor for non-muscle myosin II, was also added to the ADSC culture in combinatorial hydrogels and the gene expression of non-muscle myosin II isoforms (IIA and IIB) and osteocalcin were quantified.

2. Materials and methods

2.1. Cell culture

Human adipose-derived stem cells (hADSCs) were isolated from excised human adipose tissue from informed and consenting patients following procedures as previously described [26]. HADSCs were subcultured upon 90% confluence until passage 5 before use for all experiments in growth medium consisting of Dulbecco's minimal essential medium (DMEM, Invitrogen, Carlsbad, CA) supplemented with 10% (v/v) fetal bovine serum (FBS) (Gibco), 100 units ml^{-1} penicillin, and 100 $\mu g\ ml^{-1}$ streptomycin.

2.2. Combinatorial hydrogels

To generate combinatorial hydrogels with independently tunable biochemical and mechanical properties, both synthetic and extracellular-matrix-derived natural polymers were used. To tune the mechanical properties of hydrogels, synthetic polymer poly(ethylene glycol)-diacrylate (PEGDA) with different molecular weights (3400 or 5000) were prepared in sterile Dulbecco's phosphate-buffered saline (dPBS) and used at a final concentration of 10%, 15%, and 20% (w/v) containing photoinitiator Igracure D2959 (0.05% (w/v)) (Ciba Specialty Chemicals, Tarrytown, NY, USA). Collagen I (3.0 $mg\ ml^{-1}$, BD Biosciences, San Jose, CA, USA) was incorporated in all hydrogel compositions and mixed with PEGDA solution to reach a final concentration of 1 $mg\ ml^{-1}$, which provided adhesion sites for hADSCs to facilitate mechanosensing. To tune the biochemical properties of hydrogels, fibronectin (FN) (10 and 25 $\mu g\ ml^{-1}$) and laminin (LM) (10, 50 and 100 $\mu g\ ml^{-1}$) were interspersed in the hydrogel at different final concentrations. Specifically, FN and LN stock solutions were added to the collagen I solution prior to gelation such that they were physically entrapped and interdispersed in the hydrogel network after gelation. PEGDA hydrogels with collagen I but no FN and LM were included as control. Passage 6 hADSCs were homogeneously suspended in the hydrogel solutions with varying compositions at a cell density of 15 million ml^{-1}. The cell–hydrogel mixture (50 μl) was loaded into 96-well plates and exposed to UV light (365 nm, 4 $mW\ cm^{-2}$) for 5 minutes to induce photocrosslinking of the PEGDA network. The hydrogels were further incubated at 37 °C for 1 h to induce collagen I gelation. The resulting hydrogel microarrays consisted of 42 different compositions in total (Table 1) and all experiments were conducted in triplicates. All cell-laden hydrogels were then transferred to 24-well culture plates and cultured in the presence of osteogenic medium. Cell viability in all 42 hydrogel compositions was assessed 24 h post-encapsulation using LIVE/DEAD Cell Viability Assay Kit (Molecular Probes) with calcein-AM and ethidium homodimer following the manufacturer's protocol.

2.3. In vitro cultivation

All hydrogel samples were cultured at 37 °C in 5% CO_2 in 2 ml of osteogenic medium for 21 days. Osteogenic medium consists of high-glucose Dulbecco's modified Eagle's medium (DMEM; GIBCO), 100 nM dexamethasone (Sigma), 50 $mg\ ml^{-1}$ ascorbic acid 2-phosphate (Sigma), 10 mM β-glycerophosphate (Sigma), 10% fetal bovine serum (Gibco), 100 units ml^{-1} penicillin, and 100 $\mu g\ ml^{-1}$ streptomycin (Gibco). Medium was changed three times per week.

2.4. Mechanical testing

Unconfined compression tests were conducted using an Instron 5944 materials testing system (Instron Corporation, Norwood, MA) fitted with a 10 N load cell (Interface Inc., Scottsdale, AZ, USA). The test set-up consisted of custom-made aluminum compression platens lined with PTFE to minimize friction. Acellular hydrogels were fabricated and equilibrated in PBS solution for 24 h at room temperature prior to mechanical testing. Before each test, specimen diameter (~6 mm) and thickness (~3 mm) were measured. All tests were conducted in PBS solution at room temperature. A preload of ~5 mN was applied to ensure the hydrogel surface was in full contact with the upper platen. The upper platen was then lowered at a rate of 1% strain s^{-1} to a maximum strain of 15%. The resulting stress–strain curves were fitted with a second-order polynomial and the compressive tangent moduli were determined at strain values of 15%.

2.5. Calcium assay

Lyophilized hydrogel samples were homogenized in 0.5 M HCl and vigorously vortexed for 16 h at 4 °C. The supernatant was

Please cite this article in press as: Nii M et al. The effects of interactive mechanical and biochemical niche signaling on osteogenic differentiation of adipose-derived stem cells using combinatorial hydrogels. Acta Biomater (2012), http://dx.doi.org/10.1016/j.actbio.2012.11.002

Table 1
Compositions of combinatorial hydrogels with varying components of biochemical and mechanical properties.

		w/v	Biochemical Cues						
			FN 10			FN 25			No FN
			LM10	LM50	LM100	LM10	LM50	LM100	No LM
PEGDA	MW 3400	10%	1	2	3	4	5	6	7
Mechanical		15%	8	9	10	11	12	13	14
Cues		20%	15	16	17	18	19	20	21
	MW 5000	10%	22	23	24	25	26	27	28
		15%	29	30	31	32	33	34	35
		20%	36	37	38	39	40	41	42

Biochemical compositions were varied by changing concentration of fibronectin (FN) (0, 10 or 25 μg ml^{-1}) and laminin (LM) (0, 10, 50 or 100 μg ml^{-1}). Mechanical properties were varied by changing the molecular weight (MW) and concentration of poly(ethylene glycol) diacrylate (PEGDA) (10, 15 and 20% w/v) w/v: weight by volume percentage.

collected for calcium assay following the manufacturer's protocol (Sigma Diagnostics 587) based on the reaction of calcium with o-cresolphthalein-complexone and standard curve. The colorimetric reaction was read at 570 nm with a microplate reader.

2.6. RNA extraction and reverse transcription-polymerase chain reaction

To evaluate osteogenic differentiation and non-muscle-myosin expression, total RNA was isolated. Total RNA ($n = 3$ half gels/group) was extracted with Trizol (Aldrich) and cDNA was synthesized by reverse transcription (RT) with Superscript First Strand Synthesis System (Invitrogen, Carlsbad, CA, USA) following the manufacturer's protocol. Quantitative RT-PCR was performed using Power® SYBR Green Kit (BD Biosciences) following the manufacturer's protocol and running all samples for 40 PCR cycles on Applied Biosystems 7900 Real-Time PCR System (Carlsbad, CA, USA). The gene expression of osteocalcin, a late bone marker, and non-muscle myosin (NMM) IIA and IIB were examined. Relative expression level of target genes was determined using the comparative C_T method, where target gene expression was first normalized to an endogenous gene, GAPDH, followed by a second normalization to the gene expression level measured in the control group 28.

2.7. Histological analysis and immunofluorescence staining

Selective groups were processed for histological analysis at the end of three weeks ($n = 1$/group) based on the relative osteocalcin gene expression levels. The cell–hydrogel constructs were fixed in 4% paraformaldehyde overnight at 4 °C and transferred to 70% ethanol until embedded in paraffin according to standard histological techniques. Sections were stained with Alizarin red for calcium. For immunostaining, enzymatic antigen retrieval was performed by incubation in 0.1% Trypsin at 37 °C for 15 min. Sections were then blocked with blocking buffer consisting of 2% goat serum, 3% BSA and 0.1% Triton X-100 in 1× PBS, followed by incubation in rabbit polyclonal antibody to collagen type I, II or osteocalcin (Abcam) overnight at 4 °C and secondary antibody (Alexa Fluor 488 goat anti-rabbit) incubation for 1 h at room temperature. Nuclei were counterstained with DAPI mounting medium (Vectashield) and images were taken with a Zeiss fluorescence microscope.

2.8. Non-muscle myosin II inhibition

In order examine the role of matrix stiffness-sensing on ADSC osteogenesis, selective groups were treated with blebbistatin, a non-muscle myosin inhibitor. Specifically, blebbistatin (EMD Biosciences) was added at a concentration of 50 μM with media change every 2 days for 21 days. Blebbistatin treatment was performed on a smaller set of hydrogels focusing on the leading groups (29 and 30) as identified by evaluating the osteocalcin expression and calcium production of all the 42 hydrogel formulations. Experimental groups containing the same biochemical cues as the leading groups but varying mechanical cues (different PEGDA concentrations: groups 23 and 27; different PEGDA MW: groups 2, 9 and 16) were also included. Hydrogel group 35 with no FN or LM served as a control. Three gels were assessed per group.

2.9. Statistical testing

GraphPad Prism (Graphpad Software, San Diego, CA, USA) was used to perform statistical analysis on mechanical testing data. One- or two-way analysis of variance and pairwise comparisons with Tukey's post hoc test were used to determined statistical significance ($p < 0.05$). Data were represented as mean ± standard deviation ($n = 3$/group).

3. Results

3.1. Mechanical properties ECM hydrogel network

Unconfined compression test was performed to measure the compressive tangent moduli of the hydrogels. The collection of hydrogels exhibited a wide range of moduli, ranging from 15 to 194 kPa (Fig. 1a). Variations in the molecular weight and concentration of the PEGDA led to significant changes in compressive modulus. Increasing the PEGDA concentration (w/v%) in the hydrogel composition led to an increase in the hydrogel modulus, while increasing the PEGDA molecular weight (MW) from 3400 to 5000 decreased hydrogel modulus by ~50% (Fig. 1a). On the other hand, varying the biochemical cues did not lead to significant changes in the compressive modulus of the hydrogels (Fig. 1b).

3.2. Cell viability

Cell viability in all 42 hydrogel compositions was assessed 24 h post-encapsulation. Over 90% of the cells were viable in all hydrogel compositions with no apparent differences among different groups.

3.3. Calcium production

Mineralization was examined as an indicator of osteogenesis by measuring calcium production (Fig. 2). The results showed that every MW 5000 group had higher calcium levels per wet weight than the MW 3400 group with the same composition (Figs. 2 and S2). The data also indicated that calcium production varied non-linearly with mechanical and biochemical properties.

Please cite this article in press as: Nii M et al. The effects of interactive mechanical and biochemical niche signaling on osteogenic differentiation of adipose-derived stem cells using combinatorial hydrogels. Acta Biomater (2012), http://dx.doi.org/10.1016/j.actbio.2012.11.002

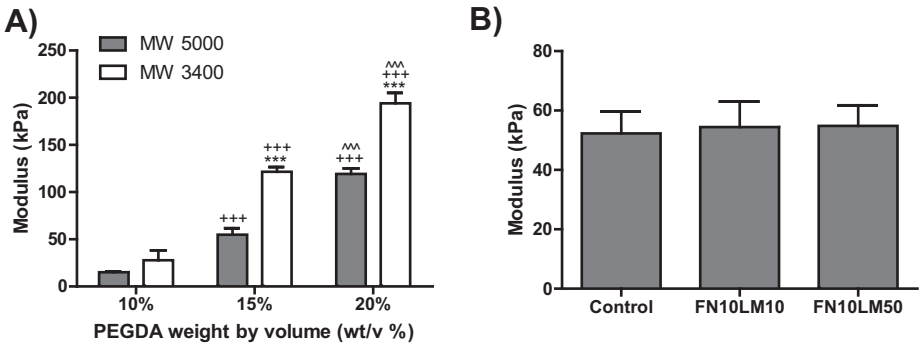

Fig. 1. Compressive tangent moduli from unconfined mechanical testing of the PEGDA polymer network. (A) Hydrogels with varying molecular weight (MW 5000 or MW3400) and concentration (10, 15 and 20% w/v) and constant biochemical cues (FN 10 μg ml^{-1} and LN 50 μg ml^{-1}). (B) Hydrogels with varying biochemical cues and constant mechanical property (MW 5000, 15% w/v). Data represented as average ± standard deviations ($n = 3$, $^{+++}p < 0.001$ compared with 10% PEGDA of the same MW, $^{\wedge\wedge\wedge}p < 0.001$ compared with 15% PEGDA of the same MW, $^{***}p < 0.001$ compared with MW 3400 of the same w/v%).

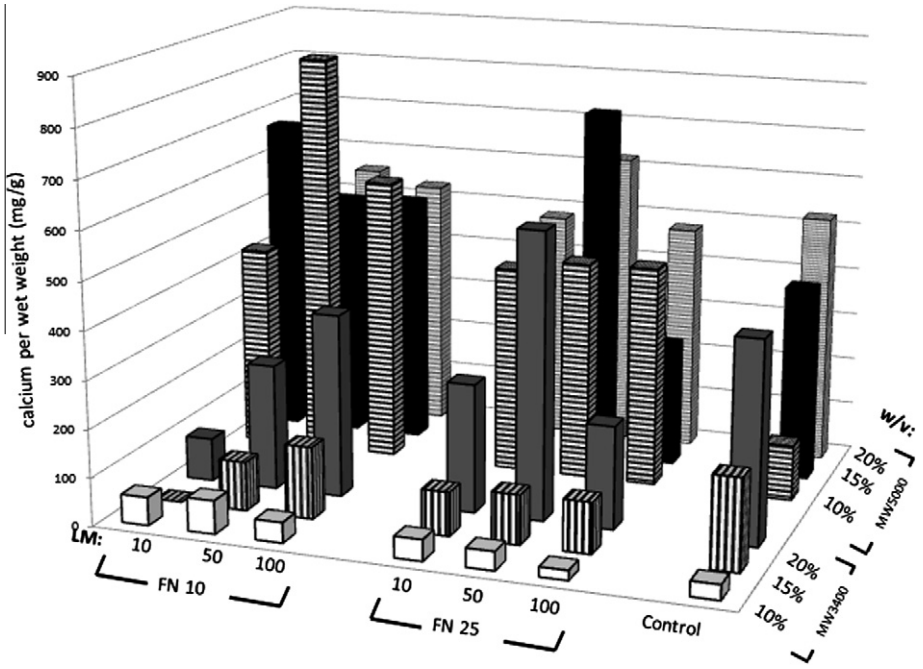

Fig. 2. Calcium production normalized by the wet weight of the scaffold (mg g^{-1}) after 3 weeks of culture in hydrogels under osteogenic conditions.

3.4. Osteocalcin gene expression

Relative osteocalcin gene expression was determined to assess the extent of ADSC osteogenesis. Osteocalcin gene expression varied drastically in different hydrogel compositions (Figs. 3 and S3). In the absence of LM and FN, osteocalcin expression increased with increasing PEGDA concentration (w/v%), peaking at 20% w/v PEGDA for both MW 3400 and MW 5000, reaching up to 58-fold and 46-fold of the control (group 28) respectively. In the presence of LM and FN, osteocalcin gene expression was generally higher in hydrogels consisting of PEGDA of MW 5000 than those of MW 3400. Furthermore, instead of peaking at 20%w/v/ PEGDA, osteocalcin expression often peaked at 15% w/v PEGDA compared with groups with the same LM and FN concentrations. Osteocalcin expression was 130–146-fold higher in the leading cluster of compositions with MW 5000, 15% w/v and 10 μg ml^{-1} FN (groups 29–31) compared to the control. Interestingly, osteocalcin expression was markedly decreased to 12–47-fold of the control when FN concentration was increased from 10 to 25 μg ml^{-1} (groups 32–34). In addition to changing the effects of PEGDA concentration on osteocalcin expression, FN concentration also altered the effects of LM on osteocalcin expression. Osteocalcin expression increased with increasing LM concentration at 10% w/v PEGDA MW 5000 with 10 μg ml^{-1} FN (groups 22–24). However, when FN concentration was increased to 25 μg ml^{-1} (groups 25–27), osteocalcin expression decreased with increasing LM concentration.

3.5. Osteocalcin staining

The hydrogel group with 10 μg ml^{-1} FN, 50 μg ml^{-1} LM and 10% PEGDA MW 5000 (group 23) at three weeks stained intensely for osteocalcin (Fig. 4A). Hydrogel groups with the same biochemical cues (10 μg ml^{-1} FN and 50 μg ml^{-1} LM) but higher PEGDA MW 5000 concentrations (15% and 20%, groups 30 and 37) also stained positively for osteocalcin (Fig. 4B and C). At 15% PEGDA MW 5000, lowering the LM concentration from 50 to 10 μg ml^{-1} while keeping the FN concentration at 10 μg ml^{-1} (group 29) resulted in comparable osteocalcin staining (Fig. 4B and D). Osteocalcin was not detected when the PEGDA molecular weight was reduced from 5000 to 3400 while the biochemical cues were kept constant

Please cite this article in press as: Nii M et al. The effects of interactive mechanical and biochemical niche signaling on osteogenic differentiation of adipose-derived stem cells using combinatorial hydrogels. Acta Biomater (2012), http://dx.doi.org/10.1016/j.actbio.2012.11.002

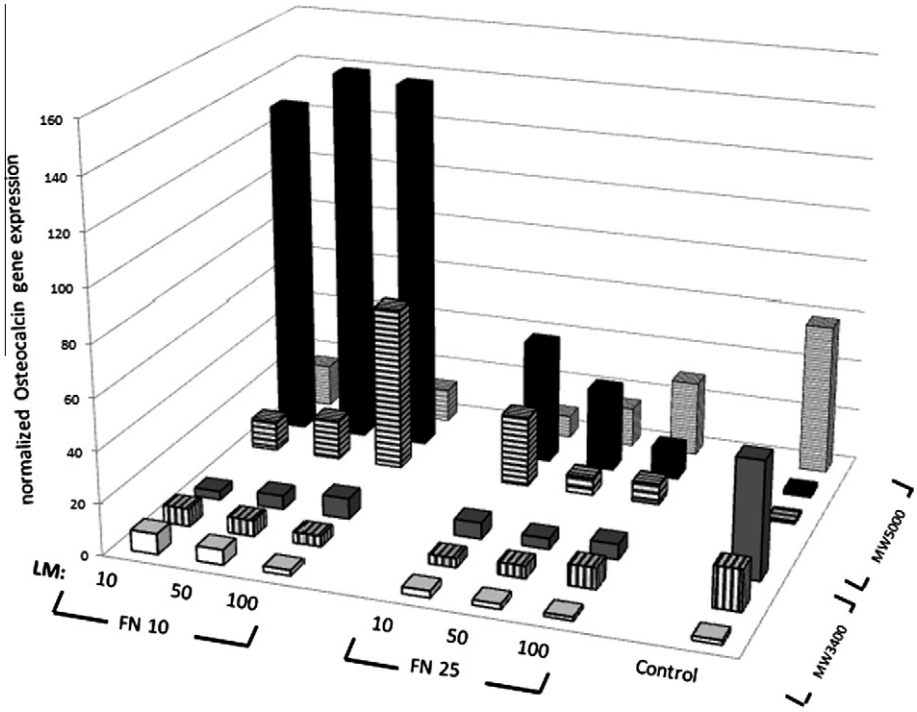

Fig. 3. Quantitative gene expression of osteocalcin, a mature bone marker, by the encapsulated human adipose-derived stem cells (hADSCs) after 3 weeks of culture in combinatorial hydrogels under osteogenic conditions. All experiments were done in triplicates and results were presented as relative fold changes in all groups and normalized to control group (10% PEGDA MW 5000, no FN, no LM).

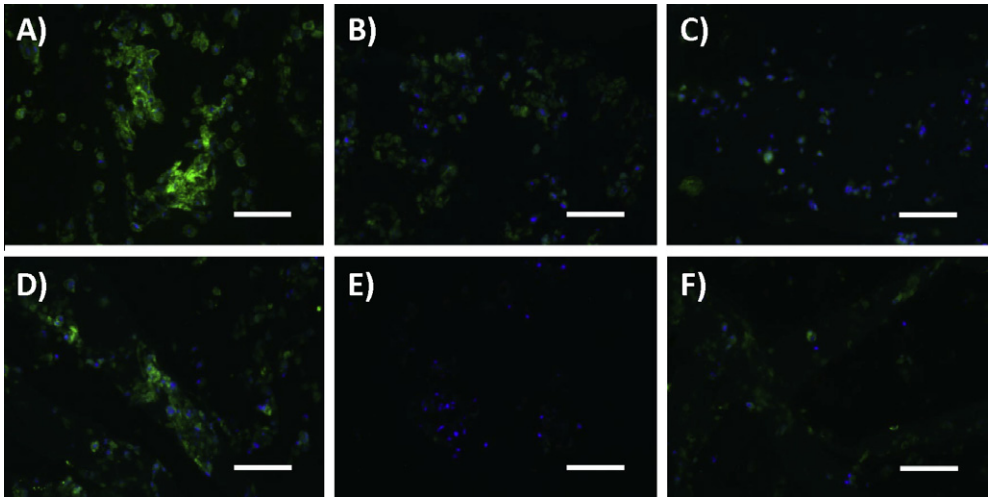

Fig. 4. Osteocalcin immunostaining after 3 weeks of hADSC culture in combinatorial hydrogels under osteogenic conditions. The ECM compositions are: (A) 10% PEGDA MW 5000, 10 μg ml^{-1} FN, 50 μg ml^{-1} LM (group 23); (B) 15% PEGDA MW 5000, 10 μg ml^{-1} FN, 50 μg ml^{-1} LM (group 30); (C) 20% PEGDA MW 5000, 10 μg ml^{-1} FN, 50 μg ml^{-1} LM; (D) 15% PEGDA MW 5000, 10 μg ml^{-1} FN, 10 μg ml^{-1} LM (group 29); (E) 15% PEGDA MW 3400, 10 μg ml^{-1} FN, 50 μg ml^{-1} LM (group 9); and (F) 15% PEGDA MW 5000, no LM, no FN (group 35). Scale bar = 100 μm.

(group 9; Fig. 4B and E). Low-intensity staining was detected in the absence of LM and FN (group 35; Fig. 4E).

3.6. Collagen I and II staining

Collagen I was stained positively in hydrogel groups at all three concentrations of PEGDA MW 5000 with 10 μg ml^{-1} FN and 50 μg ml^{-1} LM (groups 23, 30, 37; Fig. 5A–C). Lowering the LM concentration to 10 μg ml^{-1} did not reduce collagen I staining (group 29; Fig. 5D), while reducing the MW to 3400 (group 9; Fig. 5E) or eliminating both LM and FN (group 35; Fig. 5F) reduced collagen I staining. Little collagen II staining was present in all groups (Fig. S4).

3.7. Alizarin red staining

Hydrogel groups with 10 μg ml^{-1} FN, 50 μg ml^{-1} LM and 10% or 15% PEGDA MW 5000 (group 23 and 30; Fig. 6A and B) showed intense Alizarin red staining, indicating that calcium was deposited by the ADSCs. Alizarin red staining was less intense in the hydrogel group with the same biochemical composition (10 μg ml^{-1} FN and 50 μg ml^{-1} LM) but a higher PEGDA MW 5000 concentration of

Please cite this article in press as: Nii M et al. The effects of interactive mechanical and biochemical niche signaling on osteogenic differentiation of adipose-derived stem cells using combinatorial hydrogels. Acta Biomater (2012), http://dx.doi.org/10.1016/j.actbio.2012.11.002

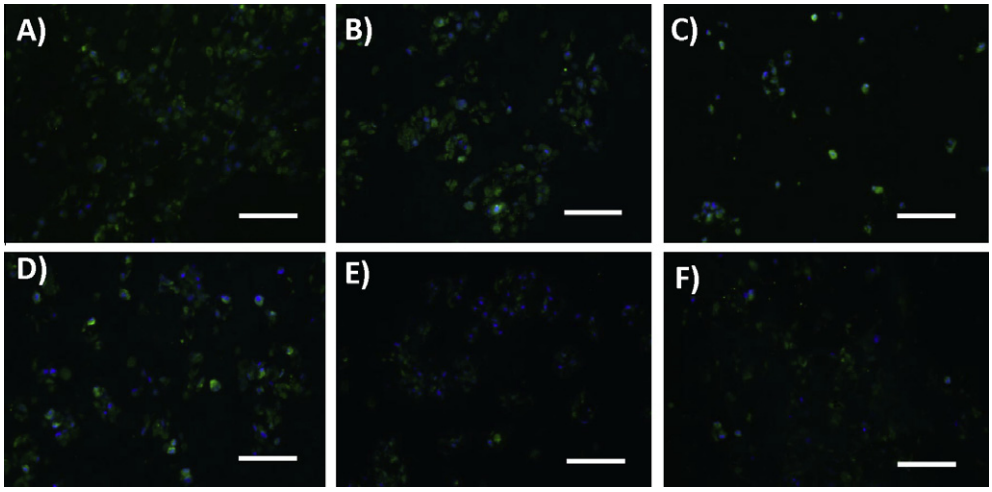

Fig. 5. Collagen I immunostaining after 3 weeks of hADSC culture in combinatorial hydrogels under osteogenic conditions. The ECM compositions are: (A) 10% PEGDA MW 5000, 10 μg ml^{-1} FN, 50 μg ml^{-1} LM (group 23); (B) 15% PEGDA MW 5000, 10 μg ml^{-1} FN, 50 μg ml^{-1} LM (group 30); (C) 20% PEGDA MW 5000, 10 μg ml^{-1} FN, 50 μg ml^{-1} LM; (D) 15% PEGDA MW 5000, 10 μg ml^{-1} FN, 10 μg ml^{-1} LM (group 29); (E) 15% PEGDA MW 3400,10 μg ml^{-1} FN, 50 μg ml^{-1} LM (group 9); and (F) 15% PEGDA MW 5000, no LM, no FN (group 35). Scale bar = 100 μm.

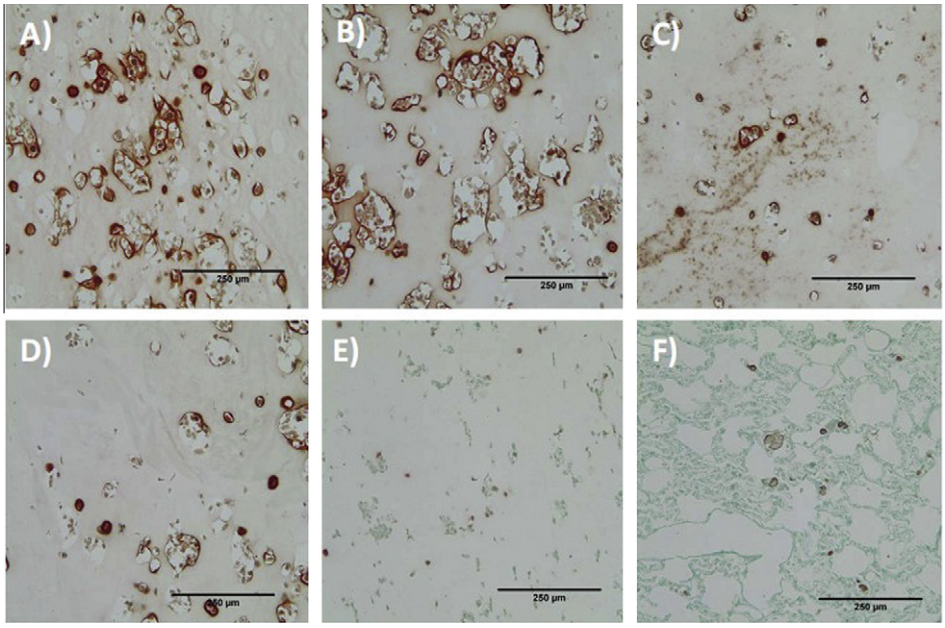

Fig. 6. Alizarin red staining after 3 weeks of hADSC culture in combinatorial hydrogels under osteogenic conditions. The ECM compositions are: (A) 10% PEGDA MW 5000, 10 μg ml^{-1} FN, 50 μg ml^{-1} LM (group 23); (B) 15% PEGDA MW 5000, 10 μg ml^{-1} FN, 50 μg ml^{-1} LM (group 30); (C) 20% PEGDA MW 5000, 10 μg ml^{-1} FN, 50 μg ml^{-1} LM; (D) 15% PEGDA MW 5000, 10 μg ml^{-1} FN, 10 μg ml^{-1} LM (group 29); (E) 15% PEGDA MW 3400, 10 μg ml^{-1} FN, 50 μg ml^{-1} LM (group 9); and (F) 15% PEGDA MW 5000, no LM, no FN (group 35).

20% (group 37; Fig. 6C). The hydrogel group with 10 μg ml^{-1} FN, 10 μg ml^{-1} LM and 15% PEGDA MW 5000 (group 29) stained positively for Alizarin red (Fig. 6D). When PEGDA with MW 3400 was substituted for MW 5000 while the biochemical compositions (10 μg ml^{-1} FN and 50 μg ml^{-1} LM) were maintained, there was little Alizarin red staining (group 9; Fig. 6E). Similarly, eliminating the FN and LM in the hydrogel (group 35; Fig. 6F) also resulted in little Alizarin red staining.

3.8. Blebbistatin gene expression

To evaluate the effect of matrix stiffness on ADSC osteogenesis, selective hydrogel groups were treated with blebbistatin to inhibit non-muscle myosin II (NMM II) activity of ADSCs. In the absence of blebbistatin treatment, NMM IIA (Fig. 7a), NMM IIB (data not shown) and osteocalcin (Fig. 7b) expression exhibited similar trends. The hydrogel group with 15% PEGDA MW 5000, 10 μg ml^{-1} FN and 50 μg ml^{-1} LM (group 30) had the highest expression in both NMM IIA and osteocalcin, exhibiting 850- and 146-higher expression than the respective hydrogel control without FN or LM (group 35). Blebbistatin treatment dramatically reduced NMM IIA and IIB expression. In hydrogel groups with 10% and 15% PEGDA MW 5000 (10 μg ml^{-1} FN, 50 μg ml^{-1} LM) (groups 23 and 30), NMM IIA expression was reduced to ~3–9% of the respective non-treated control (Fig. 7a). Similarly, osteocalcin gene expression was reduced to ~6 and 12% of the respective non-treated control in these two groups. When PEGDA concentration was further increased to 20% (group 37) or when biochemical cues

Please cite this article in press as: Nii M et al. The effects of interactive mechanical and biochemical niche signaling on osteogenic differentiation of adipose-derived stem cells using combinatorial hydrogels. Acta Biomater (2012), http://dx.doi.org/10.1016/j.actbio.2012.11.002

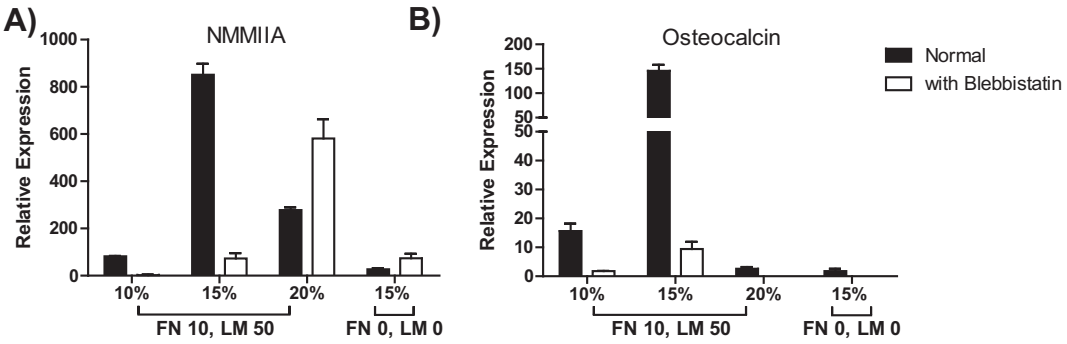

Fig. 7. Quantitative gene expression of: (A) osteocalcin and (B) non-muscle myosin IIB (NMM IIB) by hADSCs after 3 weeks of hADSC culture in combinatorial hydrogels under osteogenic conditions with and without blebbistatin treatment. All hydrogels consisted of PEGDA MW 5000 with varying PEGDA concentration, 10 μg ml^{-1} FN and 50 μg ml^{-1} LM, with the exception of the last group, with no FN and no LM. All experiments were done in triplicates and results were presented as relative fold changes in all groups using normalized mRNA level in group 35 as control.

were absent (group 35), osteocalcin expression was reduced to an undetected level with blebbistatin treatment (Fig. 7b).

4. Discussion

Here we report the development of 3-D combinatorial hydrogels with independent control of mechanical and biochemical properties to study ADSC osteogenesis. By varying PEGDA molecular weight and concentration, we obtained hydrogels with a wide range of stiffness (15 to 194 kPa), which has been shown to be relevant for bone differentiation [14,15,28]. Previous studies often focused on the effects of either mechanical or biochemical cues on cell fate and differentiation, and how these cues collectively influence stem cell fate remains unknown [4,5,7,8,28]. The combinatorial hydrogels reported herein allow for the independent tuning of mechanical and biochemical properties. Using such 3-D combinatorial hydrogel platform, we identified specific ranges of mechanical and biochemical cues that synergistically promote ADSC osteogenesis. In the absence of LM and FN, an increase in matrix stiffness resulted in enhanced bone differentiation within each molecular weight group, as shown by calcium production and osteocalcin gene expression (Figs. 2 and 3). The observed enhancement in ADSC osteogenesis with increasing matrix stiffness is consistent with previous studies which suggested that osteogenesis is favored in a microenvironment with matrix stiffness that mimics native collagenous bone tissue, which is relatively stiff (~100 kPa) [14,28,29]. Our results also showed that the optimal range of mechanical stiffness for osteogenesis depends highly on the biochemical niche cues. In the presence of LM and FN, osteocalcin gene expression peaked at intermediate matrix stiffness (groups 29–31), reaching over 140-fold higher than the control without FN or LM (group 28; Fig. 3). The striking enhancement of ADSC osteogenesis only occurred in a narrow range of biochemical (10 μg ml^{-1} FN) and mechanical cues (15% PEGDA MW 5000), and further increase in FN concentration or mechanical stiffness markedly reduced osteocalin expression. Consistent with our observation, a recent study reported enhanced osteogenic commitment of murine mesenchymal stem cells (mMSCs) at intermediate stiffness (11–30 kPa) with the presence of RGD peptides in 3-D hydrogels [15].

Our results showed that the synergistic effects of mechanical and biochemical cues on enhanced ADSC osteogenesis only occurred within a specific range. Most previous studies often optimize different niche cues sequentially, and our results suggest that optimal niche compositions are likely to be missed using such an approach. For example, if we had first optimized mechanical stiffness for osteogenesis using biochemical cues without FN or LM, we would have chosen groups with the highest stiffness (20% w/v) to further vary biochemical cues. However, our combinatorial results showed that leading groups actually occurred at intermediate stiffness (15% w/v) in the presence of additional biochemical cues. Furthermore, the effects of biochemical cues on stem cell osteogenesis may also be opposite, depending on additional biochemical or mechanical cues. For example, increasing LM concentration enhanced osteogenesis at certain mechanical properties and FN concentrations (e.g. 20% w/v MW 5000 and FN 25 μg ml^{-1}) but reduced osteogenesis at other ranges (e.g. 15% MW 5000 and FN 25 μg ml^{-1}). The absence of collagen II staining (Fig. S4) in all hydrogel compositions indicate the absence of intermediate cartilage formation. This suggests that our combinatorial hydrogels supported the ADSCs to undergo intramembranous ossification as opposed to endochondral ossification, and may be suitable for the treatment of cranial defects [5,30]. Together, our results confirm that stem cells respond to interactive niche cues in a non-linear and unpredictable manner, and highlight the necessity of examining interactive niche cues using combinatorial platforms such as the one shown in this study. While the biochemical cues were physically interlocked within the synthetic PEGDA network in our platform, which may lead to more heterogeneous presentation of biochemical ligands, future studies can incorporate biochemical cues using covalent crosslinks to achieve more precise control of biochemical ligand density and distribution.

The drastic enhancement in osteocalcin expression occurred only at a specific FN concentration (10 μg ml^{-1}) and mechanical stiffness (15% w/v MW 5000, ~55 kPa), suggesting that FN and mechanical stiffness act synergistically in enhancing ADSC osteogenesis. FN is present in bone matrix and has been implicated in osteoblast differentiation and bone morphogenesis [31,32]. Its RGD sequence can bind to cell-surface integrins and mediate cell–ECM interactions, mechanotransduction and matrix stiffness-directed differentiation [15,29]. While how FN acts in concert with matrix stiffness to regulate stem cell differentiation remains largely unknown, it has been shown that matrix stiffness can affect the strength of integrin–FN bonds [33]. In addition, cell traction force exerted by motor proteins such as myosin II can regulate the conformation as well as assembly of FN in the ECM [34,35]. In our study, changes in matrix stiffness may lead to changes in FN conformation and assembly as well as integrin–FN bond strength and organization around the cells. These changes, in turn, may mediate matrix stiffness-sensing and lead to the marked enhancement of ADSC osteogenesis observed at intermediate matrix stiffness and a specific FN concentration.

Please cite this article in press as: Nii M et al. The effects of interactive mechanical and biochemical niche signaling on osteogenic differentiation of adipose-derived stem cells using combinatorial hydrogels. Acta Biomater (2012), http://dx.doi.org/10.1016/j.actbio.2012.11.002

Non-muscle myosin II (NMMII) is an actin-binding protein that generates cytoskeletal traction and plays an important role in the mechanosensing of the cells to their microenvironment [14]. A previous study showed that NMMIIA and NMMIIB gene expression of human mesenchymal stem cells increased with increasing matrix stiffness in two dimensions [14]. In our study, we found that NMMIIA and NMMIIB expression of ADSCs in three dimensions increased when matrix stiffness increased from 10 to 55 kPa (groups 23 and 30) in the presence of biochemical cues LM and FN, but decreased with a further increase in matrix stiffness (group 37). This suggests that an optimal combination of matrix stiffness and biochemical cues may exist for enhanced NMMII expression, which subsequently influences osteogenesis. A previous 2-D study has shown that adding blebbistatin, a NMM inhibitor, led to a decrease in NMMII expression and osteogenesis [14]. We examined the effects of blebbistatin on the osteogenesis of ADSCs in three dimensions. Our results showed a decrease of over 90% in osteocalcin expression with the addition of blebbistatin, which confirms that mechano-transduction in 3-D culture plays a crucial role in the enhanced osteogenesis (Fig. 7b).

Our results also suggested that varying the molecular weight of PEGDA had an evident impact on osteogenic differentiation, with MW5000 groups performing significantly better than MW3400 counterparts for supporting ADSC osteogenesis (Figs. 2–4). Changes in molecular weight may lead to changes in mesh size and diffusion of morphogens. However, previous study has shown that changes of these properties between PEGDA MW 3400 and 5000 are negligible [36]. Chatterjee et al. reported decreased viability of osteoblasts with increasing PEGDM concentration [28], suggesting that differences in cell viability and proliferation may be responsible for the observed differences in stem cell differentiation when molecular weight of PEGDA was varied. In our study cell viability was over 90% 24 h post-encapsulation in all hydrogel compositions, with no apparent changes among various hydrogel formulations.

5. Conclusions

We developed 3-D combinatorial hydrogels with independently tunable biochemical and mechanical properties to study the effects of interactive niche cues on ADSC osteogenesis. We demonstrated that mechanical stiffness and biochemical cues interact in a non-linear manner, highlighting the importance of studying their complex interactions simultaneously. Using the combinatorial hydrogel platform, we identified that combinatorial hydrogel with intermediate stiffness (~55 kPa) and low concentration of fibronectin (10 $\mu g\ ml^{-1}$) led to an increase in osteocalcin gene expression of over 130-fold. Culture models with independently tunable niche cues could provide a powerful tool for conducting mechanistic study to uncouple complex niche cue signaling, or rapidly identifying optimal niche compositions that promote desirable cell fates. Such platforms are versatile and can be used to study various cell types or optimize niche cues for differentiation towards different lineages.

Conflicts of Interest

The authors have no conflicts to disclose.

Acknowledgements

The authors would like to thank McCormick Faculty Award Grant, Stanford Bio-X Interdisciplinary Initiative Program and Donald E. and Delia B. Baxter Foundation for funding.

Appendix A. Figures with essential colour discrimination

Certain figure in this article, particularly Figs. 4–6 are difficult to interpret in black and white. The full colour images can be found in the on-line version, at http://dx.doi.org/10.1016/j.actbio.2012.11.002.

Appendix B. Supplementary data

Supplementary data associated with this article can be found, in the online version, at http://dx.doi.org/10.1016/j.actbio.2012.11.002.

References

[1] Underhill GH, Bhatia SN. High-throughput analysis of signals regulating stem cell fate and function. Curr Opin Chem Biol 2007;11:357–66.
[2] Scadden DT. The stem-cell niche as an entity of action. Nature 2006;441:1075–9.
[3] Burdick JA, Vunjak-Novakovic G. Engineered microenvironments for controlled stem cell differentiation. Tissue Eng A 2009;15:205–19.
[4] Flaim CJ, Chien S, Bhatia SN. An extracellular matrix microarray for probing cellular differentiation. Nat Methods 2005;2:119–25.
[5] Yang F, Cho S-W, Son SM, Hudson SP, Bogatyrev S, Keung L, et al. Combinatorial extracellular matrices for human embryonic stem cell differentiation in 3D. Biomacromolecules 2010;11:1909–14.
[6] Anderson DG, Levenberg S, Langer R. Nanoliter-scale synthesis of arrayed biomaterials and application to human embryonic stem cells. Nat Biotechnol 2004;22:863–6.
[7] Soen Y, Mori A, Palmer TD, Brown PO. Exploring the regulation of human neural precursor cell differentiation using arrays of signaling microenvironments. Mol Syst Biol 2006;2:37.
[8] Yang Y, Bolikal D, Becker ML, Kohn J, Zeiger DN, Simon CG. Combinatorial polymer scaffold libraries for screening cell–biomaterial interactions in 3D. Adv Mater 2008;20:2037–43.
[9] Wakitani S, Goto T, Young RG, Mansour JM, Goldberg VM, Caplan AI. Repair of large full-thickness articular cartilage defects with allograft articular chondrocytes embedded in a collagen gel. Tissue Eng A 1998;4:429–44.
[10] Sumanasinghe RD, Bernacki SH, Loboa EG. Osteogenic differentiation of human mesenchymal stem cells in collagen matrices: effect of uniaxial cyclic tensile strain on bone morphogenetic protein (BMP-2) mRNA expression. Tissue Eng A 2006;12:3459–65.
[11] Abbott A. Cell culture: biology's new dimension. Nature 2003;424:870–2.
[12] Webb K, Li W, Hitchcock RW, Smeal RM, Gray SD, Tresco PA. Comparison of human fibroblast ECM-related gene expression on elastic three-dimensional substrates relative to two-dimensional films of the same material. Biomaterials 2003;24:4681–90.
[13] Cukierman E, Pankov R, Stevens DR, Yamada KM. Taking cell–matrix adhesions to the third dimension. Science 2001;294:1708–12.
[14] Engler AJ, Sen S, Sweeney HL, Discher DE. Matrix elasticity directs stem cell lineage specification. Am J Physiol Cell Physiol 2006;126:677–89.
[15] Huebsch N, Arany PR, Mao AS, Shvartsman D, Ali OA, Bencherif SA, et al. Harnessing traction-mediated manipulation of the cell/matrix interface to control stem-cell fate. Nat Mater 2010;9:518–26.
[16] Rowlands AS, George PA, Cooper-White JJ. Directing osteogenic and myogenic differentiation of MSCs: interplay of stiffness and adhesive ligand presentation. Am J Physiol Cell Physiol 2008;295:C1037–44.
[17] Drury JL, Mooney DJ. Hydrogels for tissue engineering: scaffold design variables and applications. Biomaterials 2003;24:4337–51.
[18] Mazzoccoli JP, Feke DL, Baskaran H, Pintauro PN. Mechanical and cell viability properties of crosslinked low- and high-molecular weight poly(ethylene glycol) diacrylate blends. J Biomed Mater Res A 2010;93A:558–66.
[19] Hern DL, Hubbell JA. Incorporation of adhesion peptides into nonadhesive hydrogels useful for tissue resurfacing. J Biomed Mater Res A 1998;39:266–76.
[20] Yang F, Williams CG, Wang DA, Lee H, Manson PN, Elisseeff J. The effect of incorporating RGD adhesive peptide in polyethylene glycol diacrylate hydrogel on osteogenesis of bone marrow stromal cells. Biomaterials 2005;26:5991–8.
[21] Hynes RO, Yamada KM. Fibronectins: multifunctional modular glycoproteins. J Cell Biol 1982;95:369–77.
[22] Keselowsky BG, Collard DM, Garcia AJ. Integrin binding specificity regulates biomaterial surface chemistry effects on cell differentiation. Proc Natl Acad Sci USA 2005;102:5953–7.
[23] Yao L, Damodaran G, Nikolskaya N, Gorman AM, Windebank A, Pandit A. The effect of laminin peptide gradient in enzymatically cross-linked collagen scaffolds on neurite growth. J Biomed Mater Res A 2010;92A:484–92.
[24] Gronthos S, Simmons PJ, Graves SE, Robey PG. Integrin-mediated interactions between human bone marrow stromal precursor cells and the extracellular matrix. J Bone Miner Res 2001;28:174–81.
[25] Hidalgo-Bastida LA, Cartmell SH. Mesenchymal stem cells, osteoblasts and extracellular matrix proteins: enhancing cell adhesion and differentiation for bone tissue engineering. Tissue Eng B Rev 2010;16:405–12.

Please cite this article in press as: Nii M et al. The effects of interactive mechanical and biochemical niche signaling on osteogenic differentiation of adipose-derived stem cells using combinatorial hydrogels. Acta Biomater (2012), http://dx.doi.org/10.1016/j.actbio.2012.11.002

[26] Zuk PA, Zhu M, Mizuno H, Huang J, Futrell JW, Katz AJ, et al. Multilineage cells from human adipose tissue: implications for cell-based therapies. Tissue Eng A 2001;7:211–28.
[27] Gimble JM, Katz AJ, Bunnell BA. Adipose-derived stem cells for regenerative medicine. Circ Res 2007;100:1249–60.
[28] Chatterjee K, Lin-Gibson S, Wallace WE, Parekh SH, Lee YJ, Cicerone MT, et al. The effect of 3D hydrogel scaffold modulus on osteoblast differentiation and mineralization revealed by combinatorial screening. Biomaterials 2010;31:5051–62.
[29] Shih YR, Tseng KF, Lai HY, Lin CH, Lee OK. Matrix stiffness regulation of integrin-mediated mechanotransduction during osteogenic differentiation of human mesenchymal stem cells. J Bone Miner Res 2011;26:730–8.
[30] Cowan CM, Shi YY, Aalami OO, Chou YF, Mari C, Thomas R, et al. Adipose-derived adult stromal cells heal critical-size mouse calvarial defects. Nat Biotechnol 2004;22:560–7.
[31] Stein GS, Lian JB, Owen TA. Relationship of cell growth to the regulation of tissue-specific gene expression during osteoblast differentiation. FASEB J 1990;4:3111–23.
[32] Winnard RG, Gerstenfeld LC, Toma CD, Franceschi RT. Fibronectin gene expression, synthesis and accumulation during in vitro differentiation of chicken osteoblasts. J Bone Miner Res 1995;10:1969–77.
[33] Friedland JC, Lee MH, Boettiger D. Mechanically activated integrin switch controls alpha5beta1 function. Science 2009;323:642–4.
[34] Smith ML, Gourdon D, Little WC, Kubow KE, Eguiluz RA, Luna-Morris S, et al. Force-induced unfolding of fibronectin in the extracellular matrix of living cells. PLoS Biol 2007;5:e268.
[35] Lemmon CA, Chen CS, Romer LH. Cell traction forces direct fibronectin matrix assembly. Biophys J 2009;96:729–38.
[36] Cruise GM, Scharp DS, Hubbell JA. Characterization of permeability and network structure of interfacially photopolymerized poly(ethylene glycol) diacrylate hydrogels. Biomaterials 1998;19:1287–94.

Please cite this article in press as: Nii M et al. The effects of interactive mechanical and biochemical niche signaling on osteogenic differentiation of adipose-derived stem cells using combinatorial hydrogels. Acta Biomater (2012), http://dx.doi.org/10.1016/j.actbio.2012.11.002